# Production and investigation of single photon source nanocrystals doped with rare-earth metals (PD134921)

## Final report

### Foreword

Single-photon sources are considered as one of the possible means of secure information transport and quantum information processing. Nanocrystals prepared from rare-earth (RE) ion doped single crystals can potentially play an important role in coherent quantum optical experiments where the rare-earth dopant can act like single-photon source. There are several conditions for such an operation mode: (1) The concentration of the dopant atoms must be low, only a few of them are allowed to be present in each nanocrystal; therefore, if the optical cross-section of the nanocrystals do not overlap, it is possible to excite only one atom (ion) with a focused laser beam. (2) The light scattered by dopant atoms has to be collected with high efficiency.

The goal of this work was the production and investigation of rare-earth doped nanocrystals – (with the size of 10 nm or less) using a well-defined, reproducible method – which are suitable for single photon source.

### 1. Preparation of lithium niobate nanocrystals doped with Yb, Tm, Dy, Er

#### *1.1. Wet milling method*

RE (Tm, Dy, Er, Yb) doped lithium niobate nanocrystals were successfully prepared by co-milling RE oxides with sintered (800°C, 3h) lithium niobate ($LiNbO_3$, LN) powder and by grinding RE doped LN single crystal by high-energy ball milling method. When the starting materials of the co-milling were $Nb_2O_5$, $Li_2O$ and $RE_2O_3$, RE-niobate appeared in the product instead of RE doped LN. The samples were ground by a Fritsch Pulverisette 7 Premium line planetary mill in a zirconia vial with 70 g zirconia balls in diameter of 3, 0.5 and 0.1 mm. The system was equipped with an EASY GTM Gas Pressure and Temperature Measuring System in order to avoid damage caused by overheating or excessive pressure. The set limit was 70°C for all milling. With our method (grinding for 1 minute, waiting for 10 minutes), neither the pressure nor the temperature exceeded the set value even during 100 cycles of grinding. The rotation rate was 1100 rpm, while the load was 5 g powder and 10 ml distilled water in each case. The residue of RE-oxide was removed by washing the milled powder by 15% $HNO_3$ solution. The incorporation of the RE ion into the $LiNbO_3$ lattice was detected by photoluminescence or absorption spectroscopy. Formed phases were identified by X-ray diffraction phase analysis. The concentration of the dopant and the size distribution of the particles were investigated by Scanning Electron Microscope (SEM) mapping, Energy-Dispersive X-ray Spectroscopy (EDS) and Dynamic Light Scattering (DLS) methods and the final average size of the particles diameter obtained by these methods was 5-15 nm [1].

Lithium niobate nanocrystal co-doped with two different RE ions (in this case: Yb and another rare-earth metal) was prepared in the same way (co-milling the sintered LN powder or pure LN single crystal by the RE-oxides). The process was described above.

Due to the loss of $Li_2O$, the produced suspension was alkaline (pH = 12-14) and dissolved the $ZrO_2$ material of the crucible and the milling balls. The presence of Zr in the nanorcrystal was proved by EDS measurements.

Lithium yttrium borate (LYB) as a host material was also tried but the suspension of the wet milled LYB was much more alkaline than the LN and the crucible and the milling balls were strongly damaged. In addition, LYB is a hygroscopic material, so it significantly lost its crystalline structure during the aqueous milling process. In this case dry milling in inert atmosphere can be tried but this type of grinding crucible was not available in our laboratory.

### *1.2. Dry milling method and milling in organic solvents*

For the elimination of the Zr dissolution into the sample dry milling was tried. In this case there was no solvent in the system. The parameters of the optimized method were the same as those for the wet milling except of the size of the milling balls. The size of the milled particles didn't decrease with decreasing the size of the balls (3 to 0.1 mm) because the particles stuck together, so only the balls with the diameter of 3 mm could be used in the optimized milling method. With this method the dissolution of Zr could be eliminated while the average diameter of the particles was about 45 nm [2].

The substitution of water by different organic solvents (ethylene-glycol, TritonX-100) was tried also in order to eliminate the alkaline properties and the dissolution of Zr. The amount of the added solvent was changed from 10 ml to 0.1 ml. In all these cases the sample was not milled at all because the friction force was so weak that the milling efficiency was not sufficient.

## 2. Rare-earth ion loss of Er- or Yb-doped $LiNbO_3$ crystals due to mechanical destructive effect of high-energy ball milling

For developing a well-defined and reliable method to produce particles with a diameter of about 10 nm containing the rare-earth dopant(s) in a predetermined concentration and in such a dilute form so that the optically active atoms are far enough from each other to behave as non-interacting optically active centres, the wet milling method seems to be ideal.

What still needs to be paid attention to is the structural change due to the mechanical effect, since the knowledge of the crystal structure and the surroundings of the rare-earth ion is essential for further applications.

Yb- or Er-doped LN samples were ground by zirconia balls in diameter of 3 mm with the above described optimized wet milling conditions. The milling time varied between 10-100 minutes. 1 ml portions of the suspension were taken out from the samples for characterization. The mass of the missing material was replaced with distilled water in order to keep the charge/milling balls mass ratio constant. A new sample was loaded after every second sampling in order to avoid the error due to dilution.

It was concluded from the DLS measurements, that after 30 minutes grinding time, the size distribution of the particles didn't not change and the final size of the particles were 50-70 nm (which can be explained by the fact that the size of the grinding balls was not reduced during grinding).

Phases appearing during the grinding process of the RE-LN samples were investigated on the as-received and dried suspension samples by X-ray powder diffraction method. In the RE-LN samples ground for 10 minutes, mainly the LN phase is present. During further mechanical treatment, a new phase appeared gradually with the increasing grinding time, identified as $RE_2O_3$.

Absorption spectra corresponding to the $^2F_{7/2} \longrightarrow {}^2F_{5/2}$ of the $Yb^{3+}$ ion and the $^4I_{15/2} \longrightarrow {}^4I_{11/2}$ transition of the $Er^{3+}$ ion were recorded at 9 K for each sample. The integrated area under the absorption peaks is directly proportional to the number of the absorbing ions. So the variation of the amount of ions in the same environment could be monitored with this parameter.

It could be concluded that (similarly to the Li loss of the LN crystal during high-energy ball milling process) the RE ions in Li sites are also leaving the lattice. Since the particle size distribution didn't change after 30 minutes of grinding, the samples milled for 30-100 minutes can be compared well with each other and any change is caused solely by the mechanical force. Since the $RE^{3+}$ ion loss occurs on the surface of the particles, we can say that during the grinding process, the $RE^{3+}$ ions migrate from the inner part of the 40-60 nm particles towards the surface (despite the fact that the size of the $RE^{3+}$ ion is much larger than that of $Li^+$). The behaviour of $Yb^{3+}$ and $Er^{3+}$ ions were found to be very comparable, as expected from their very similar chemical properties, size and position in the crystal lattice.

Both the $Yb^{3+}$ and $Er^{3+}$ loss of the LN matrix during the grinding process with the given parameters (1100 rpm, 10 minutes, 3 mm ball diameter) were consistent and can be described by a $0.8^{t/10\ min}$ function where $t$ is the grinding time in minutes. The curves of the different RE ions overlapped each other independently from their quantity in the samples. After 100 minutes of wet grinding with 1100 rpm of the RE-LN samples, roughly 90% of the RE content left the crystalline structure in $RE_2O_3$ form [3, 4].

Raman measurements were also made on the samples. Our device is equipped with a 633 nm laser. The Raman band of $LiNbO_3$ can be found in the 200-800 $cm^{-1}$ region. Unfortunately, in the collected spectrum the strong luminescence of $Er^{3+}$ is masked the Raman bands. For $Yb^{3+}$ a wide and weak Raman band appeared at about 400 $cm^{-1}$ which was found to be unsuitable for determining phase ratios.

## 3. Rare-earth ions in $LiNbO_3$ nanocrystals from the view of spectroscopic and force-field calculation

The results of the above described absorption measurements and theoretical calculations on $Yb^{3+}$ or $Er^{3+}$ doped LN nanocrystals were compared. Out-diffusion of the RE ions from the nano-LN particle and the appearance of an unordered phase have been concluded from the experimental results. GULP software has been used to make force-field calculations on a $Li_{245}Nb_{245}O_{735}$ unit to model the nano-LN structure containing RE dopants.

The three-dimensional energy maps as the function of the position of $RE^{3+}$ ion were sliced into different planes to interpret the results more easily. The energies in these layers were plotted as colour maps (Figure 1.), where the black dots correspond to positions of investigated $RE^{3+}$ ions.

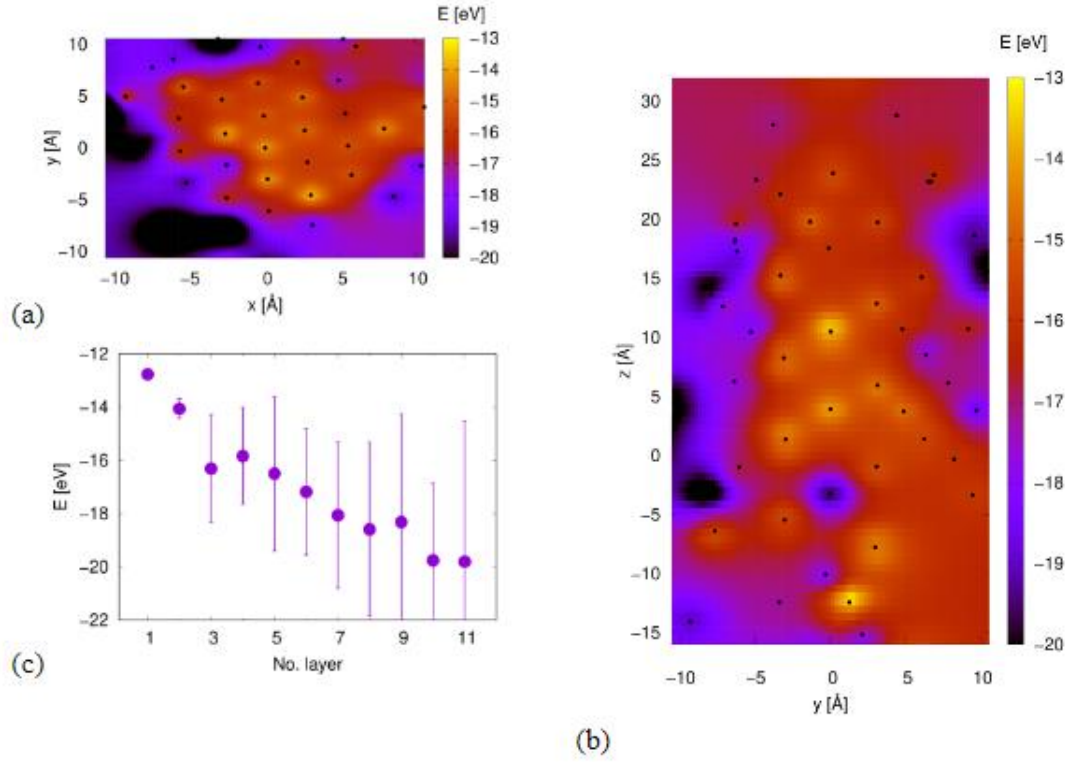


Figure 1.: Energy plot to the projection of X-Y (a) and Y-Z (b) planes with a volume thickness of about 5 Å in the center section of the nano-LN containing a single $Er^{3+}$ ion. Energy statistics of the nano-LN:Er system calculated for the 11 ellipsoid layers (c) with increasing radius.

It seems from the X-Y plane (Figure 1.a) in a 5 Å thick z-cut projection from the middle of the particle that the energy of the system decreases slightly when rare-earth ions move away from the centre and it is the lowest near the surface or inside the shell part. The projection of the Y-Z plane (Figure 1.b) shows a similar behaviour in the entire length of the nanoparticle. For a more detailed analysis, 11 ellipsoid layers were defined and statistics for these regions were determined and plotted in Figure 1.c. The analysis shows again that the average energy of nano-LN decreases as the rare-earth ions are located further off the centre. [5, 6]

## 4. Preparation of lithium niobate nanocrystals by solvothermal method

Beside the high-energy ball milling method, an easy and relatively low-temperature solvothermal process was also optimized for preparing $LiNbO_3$ nanocrystals. The effects of polyol media (ethylene-glycol, diethylene-glycol, triethylene-glycol and glycerol), reaction time (24, 48, 72 hours) and Li excess (Li/Nb = 1, 1.25, 1.5) of the starting reagents were investigated. The size and the shape of the LN particles were characterized by scanning electron microscopy. The particle size distribution was narrow and under 100 nm with homogeneous

particle size distribution for all cases. According to the X-ray diffraction phase analysis, $Li_3NbO_4$ and $Nb_2O_5$ have also been detected beside the LN phase in many samples depending on the ratio of the starting components and the reaction time. Independently of the polyol medium used, the lithium oxide uptake of the niobium(V) oxide grains stated with the formation of a lithium-rich phase, $Li_3NbO_4$, very likely at the $Nb_2O_5$/solvent boundary, which was followed by the equilibration of the concentrations within the grains. For the accomplishment of the $LiNbO_3$ formation, a lithium oxide excess was necessary. The best yield (90%) and the most homogeneous LN phase could be prepared by using diethylene glycol medium with a Li/Nb ratio of 1.5 and a 72-hour reaction time [7, 8, 9].

Yb-doped $LiNbO_3$ nanoparticles have also been attempted to be prepared by this method. The $Yb_2O_3$ was diluted in $HNO_3$, after mixed by the $Nb_2O_5$ powder and heat treated at 500 $^oC$ for 1 hour in order to eliminate the nitrate compounds. The preparation was performed with the optimized solvothermal method described above (instead of pure $Nb_2O_5$, Yb/Nb oxide mixture was used). According to the absorption measurements the whole amount of Yb was found in the form of Yb-niobate.

## 5. Deposition of the doped nanoparticles on a metal surface using a galvanic bath

Rotating Disc Electrode method was optimized for producing a homogeneous nickel surface on a Si disc with well-defined thickness containing separated nanoparticles not only on the surface but incorporated into the coating giving a possibility for facilitating the further investigations of the nanomaterial. With this method, the preliminary purification step of the raw ground material could be omitted.

Galvanic bath (containing Ni) were prepared for depositing the nanoparticles onto a Ni coated Si surface. Electric current and process time were optimized for a two-step method: the first was making 50 nm thick Ni coating on a Si plate and the second was a 50 nm thick sample containing Ni coating on the Ni coated Si plate. Particles stacked to the surface were eliminated by using an ultrasound bath during 10 minutes. The thickness, morphology and the deposition of the $LiNbO_3$ nanocrystal on the Ni surface were followed by SEM measurements.

The first experiments were carried out using a neutral Ni bath (pH = 6.5). The components were: $NiSO_4$, Saccharine, Na-lauryl-sulphate, boric acid and distilled water. The coating process was successful, the optimized parameters were: 14 $mA/cm^2$, 21 s. The sample particles were embedded into the Ni surface which was proved by SEM (figure 2.). The suspension containing sample was alkaline (as it has already been mentioned above) so the sample particles were stacked together and precipitated overnight.

(a) (b)

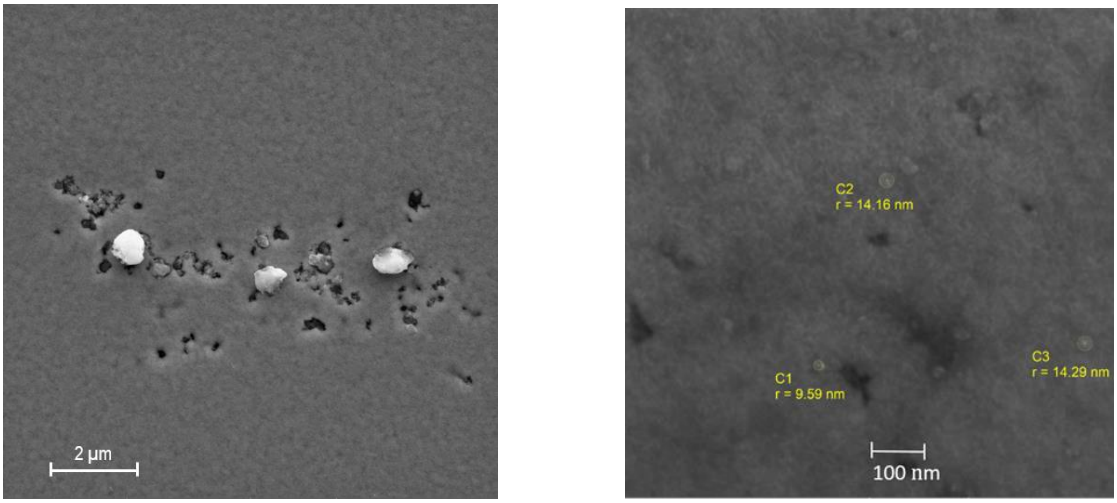


Figure 2.: SEM picture of LN nanoparticles of 70-100 nm (a) and 5-15 nm (b) embedded in the Ni surface.

In order to avoid the coagulation of the particles another Ni containing galvanic bath (form: $NiSO_4$, Saccharine, Na-citrate, ammonia solution and distilled water) was prepared with the pH of about 10. The coating process was optimized for this case too and the parameters were determined as 30 $mA/cm^2$, 29 s. The thickness of the coating was calculated from Scanning Electron Microscopic measurement as 100 nm for the Ni and 50 nm for the sample containing Ni. The particles were found embedded in the surface separately with the diameter of 15-25 nm [10, 11].

A new method was also developed for Ni coating using another electrochemical process. Using a different layout, where the cathode is in the bottom of the solution, we can help the particles settling and sticking into the surface against the electrostatic repulsion between the alkaline particles and the cathode.

## 6. Examination of the RE-LN nanocrystals by confocal microscope

In the second year of the project we have studied two types of doped lithium niobate (LN) crystals and nanocrystals: (1) LN co-doped with ytterbium and thulium atoms; (2) LN doped with erbium atoms. In LN:Yb:Tm we reported last year that the single wavelength excitation (980 nm) of the $Yb^{3+}$ ions did not yield appreciable signal from the $Tm^{3+}$ ions, due to large (order of $1cm^{-1}$) incoherent broadening of the $Yb^{3+}$ ion's absorption band. Hence it is very unlikely that at least two $Yb^{3+}$ ions in the close vicinity of a $Tm^{3+}$ ion have overlapping resonance excitation frequency, i.e. they agree within the megahertz range homogeneous linewidth. We tried to modulate the frequency of the exciting laser by means of an acousto-optic modulator but it still did not yield an observable signal from the $Tm^{3+}$ ions. The modulation range in our setup is 0-100 MHz. Hence our conclusion is that we need to apply a pulsed laser source with pulse duration in the picosecond range. In fact, the fluorescence of $Tm^{3+}$ ions in co-doped LN:Yb:Tm crystals was discovered with such pulsed excitation of the $Yb^{3+}$ ions. We started a collaboration with another laboratory of the HUN-REN Wigner RCP

which has a tuneable Ti:Sa laser. We connect the two labs with an optical fibre to transfer the pulsed laser light to the confocal microscope setup. After spectral filtering, we aim at 10-20 ps long pulses, which has a spectral bandwidth equal to the inhomogeneous broadening of the 980 nm transition of the $Yb^{3+}$ ions in LN.

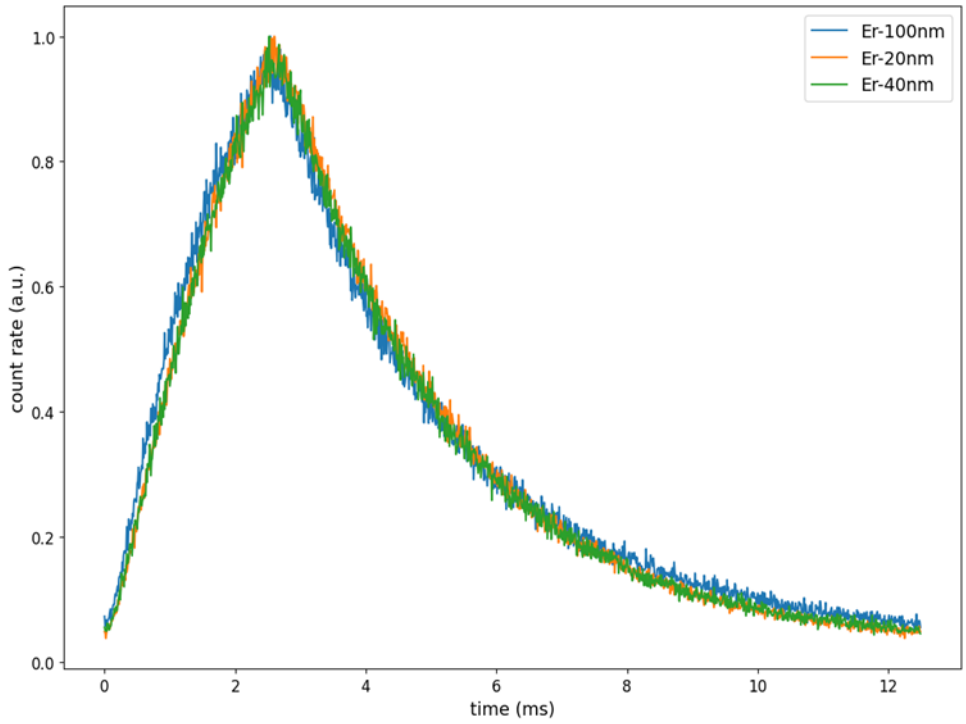


Figure 3.: The excitation-decay fluorescence histogram of $Er^{3+}$ ions in LN nanocrystals. Labels show the nanocrystal size.

The other material under study was LN:Er. We have excited the $^4I_{11/2} \longrightarrow {}^4I_{15/2}$ transition of the $Er^{3+}$ ions. After a subsequent nonradiative process the ions decay to the $^4I_{13/2}$ state. Then they decay further to the ground state by emitting a 1.5 μm photon. We observed this radiation with an SNSPD (Superconducting Nanowire Single Photon Detector) detector. We have also measured the overall decay time of the $^4I_{15/2} \longrightarrow {}^4I_{13/2} \longrightarrow {}^4I_{11/2}$ transition chain. We have performed this measurement both in bulk and nanocrystal samples. The diameter of the nanocrystals were d50 = 20 nm, 40 nm, 60 nm, 100 nm. In all cases we could get appreciable signal to determine the decay time of the transition chain. The time correlated single photon counting (TCSPC) histogram is shown in Fig. 3. The lifetime is rather long, ≃2.6 ms, hence it is very difficult to observe the fluorescence of a single $Er^{3+}$ ion: taking into account the necessary excitation time of the ions the whole process (excitation+decay) takes of the order of 4-5 ms, thus the maximum photon emission rate would be 250 Hz. The best achievable photon counting rate is 7 $s^{-1}$, because the overall photon collection efficiency of the microscope + SNSPD system is approximately 3%. This is much lower than the dark count rate of the SNSPD detector, which is about 100 $s^{-1}$.

In the course of the above experiments we observed green radiation from the bulk sample. This green light is the result of a two-photon excitation process in the $Er^{3+}$ ions. We have performed fluorescence lifetime measurement on the samples for the $^2H_{11/2}$ and $^4S_{3/2}$ energy levels and obtained 65 μs. This is quite promising, we expect that we can observe the green fluorescence even from single nanocrystals.

## Summary

During the duration of this OTKA project (2020-2023) two very serious, unforeseen difficulties were arose. Several months of forced break due to a worldwide pandemic disease and the cold laboratories because of the energy crisis in the year after were also hindered the experimental work. I would like to thank to the NKFIH-OTKA committee for the 6-month extension to submit the professional report. Although an article is still under review, the experimental work has been done.

The objectives set out in 6 points at the beginning of the project were achieved. All the planned research methods were used during the experiments. The results were presented at several conferences mainly as oral presentations. Two articles have been published in peer-reviewed journals and one manuscript is submitted.

The planned experiments were expanded by developing a new method for producing LN nanocrystals, by investigating the mechanical effect on the structure and composition of the doped nanocrystals and by computer modelling of its structure.

## References


[1] G. Dravecz, L. Kocsor, L. Péter: Preparation of nanoscaled $LiNbO_3$ doped with different RE ions by high-energy ball milling method, ICOOPMA EURODIM international conference, July 3-8, 2022, Ghent, poster presentation

[2] G. Dravecz, L. Kocsor, L. Péter, L. Kovács, Zs. Kis: Preparation of rare-earth-doped Lithium niobate nanocrystals by ball milling method, ICDIM 2020 international conference, November 23-27, 2020, online oral presentation

[3] G. Dravecz, L. Péter, T. Kolonits, K. Lengyel: Crystal structure variation of rare-earth-doped $LiNbO_3$ during milling, ICCGE 20 International Conference, July. 30 - Aug. 4., 2023, Naples, Italy, 2023, oral presentation

[4] G. Dravecz, L. Kocsor, L. Péter, L. Temleitner, D. Gál, K. Lengyel: Rare-Earth Ion Loss of Er- or Yb-Doped $LiNbO_3$ Crystals Due to Mechanical Destructive Effect of High-Energy Ball Milling, Crystals, 14(3), 223, 2024, article

[5] K. Lengyel, L. Kocsor, Zs. Kis, L. Péter, G. Dravecz: Rare-earth ions in $LiNbO_3$ nanocrystals from the view of spectroscopy and force-field calculations, Physica Status Solidi a, under review, submitted article

[6] K. Lengyel, G. Dravecz, L. Kocsor, Z. Kis, L. Péter: Rare-earth ions in $LiNbO_3$ nanocrystals from the view of spectroscopic and force-field calculation, EMRS Fall Meeting, Sept. 18-21., 2023, Warshaw, 2023, oral presentation

[7] G. Dravecz, T. Kolonits, L. Péter: Preparation of nanoscaled $LiNbO_3$ by solvothermal synthesis, International Workshop on Polar Oxides: Lithium Niobate and Related Compounds, May 11 - 13, 2022, Goslar, oral presentation

[8] G. Dravecz, T. Kolonits, L. Péter: Formation of $LiNbO_3$ Nanocrystals Using the Solvothermal Method, Crystals 13(1) 77, 2023, article

[9] G. Dravecz, K. Lengyel, L. Péter, L. Kocsor, Z. Kis: Comparing the solvothermal synthesis and high-energy ball milling methods for preparing nanoscaled $LiNbO_3$ doped with different RE ions, EMRS Fall Meeting, Sept. 18-21., 2023, Warshaw, Poland, 2023, oral presentation

[10] G. Dravecz, L. Péter: Electrodeposition of Ni / lithium niobate nanoparticles composite coatings for quantum optical applications, 14$^{th}$ International Workshop on Electrodeposited Nanostructures international conference, June 9-11, 2022, Krakow, poster presentation

[11] G. Dravecz, L. Péter: Preparation of nanostructured $LiNbO_3$ containing nickel surface on silicon carrier by rotating disc electrode method, Nanotech France 2022, June 15-17, 2022, Paris, oral presentation